

Ultrafast Femtosecond Relaxation Processes in Luminescent and Nonluminescent Conducting Polymers

J.D. Huang¹, S.V.Frolov¹ and Z.V.Vardeny¹
W.Chen² and T.J.Barton², R.Sugimoto³, M.Ozaki³ and K.Yoshino³

¹Department of Physics, University of Utah, Salt Lake City, UT84112, U.S.A.,

²Department of Chemistry, Iowa State University, Ames, Iowa, U.S.A.,

³Department of Electronic Engineering, Faculty of Engineering, Osaka University,
Osaka565, Japan

ABSTRACT:

We have employed the time-resolved photomodulation (PM) technique to study the photoexcitation dynamics in a luminescent (Si-PT) and nonluminescent ($s\text{-(CH)}_x$) conducting polymers in the low signal limit. In each polymer, we identify two exponential decay processes in the PM decay, with characteristic time constants T_1 and T_2 , where T_1 is of order 1 ps and T_2 depends on the specific polymer; T_2 in Si-PT is about 50ps, whereas T_2 in $s\text{-(CH)}_x$ is about 5ps. The difference in T_2 is tentatively attributed to radiative and non-radiative recombination kinetics, respectively. We also found that the PM decay does not show any obvious temperature and intensity dependences, whereas the polarization memory decay is longer at low temperatures.

Keywords: femtosecond spectroscopy, pump-and-probe technique, luminescent and nonluminescent conducting polymers, PM decay, polarization memory, bi-exponential response.

1. INTRODUCTION:

Conducting polymers have been extensively studied for the past 20 years because of their potential applications as conducting and semiconducting organic materials in opto-electronic devices. In general, the conducting polymers can be divided into two large classes^[1]: (i) luminescent and (ii) nonluminescent polymers. In this study, we investigate and compare the ultrafast relaxation processes in luminescent: Si-bridged polythiophene (Si-PT), and nonluminescent: monosubstituted polyacetylene ($s\text{-(CH)}_x$). We note that Si-PT^[2] is quite unique with respect to other luminescent polymers, namely, it shows a broad photoluminescent (PL) in the near infra-red spectral region extending from 1.25 eV to 1.65 eV. At the

same time when doped with I₂ vapor, Si-PT conductivity can reach ~ 500s/cm. On the other hand, (s-CH)_x has a very low photoluminescence (PL) quantum yield η ($\eta < 10^{-5}$)⁽³⁾ and is characterized by a degenerate ground state.

2. EXPERIMENTAL

In our studies, we have measured the photo modulation response dynamics of both polymers in the femtosecond and picosecond time scales in the low signal limit. We employed a colliding pulse mode-locked dye laser (CPM) with a bandwidth of about 70 Å at a center wavelength of 625 nm. The output pulse train of the CPM laser had a repetition rate of ~100 MHz, pulse duration of 100fs, and typical pulse energy of 100pJ. We applied a time-resolved pump-and-probe correlation technique in both single and double modulation configurations [4],[5].

Fig. 1 shows schematically the experimental setup. In the single modulation configuration the pump beam was modulated by an acousto-optic modulator at 4 MHz and the probe beam remained unmodulated. In the double modulation configuration, in addition to the modulation of pump beam (at 4 MHz), the probe beam was also modulated with a mechanical chopper at 1 kHz. The relative magnitude of the samples' optical transmission, $\Delta T/T$, was measured by using a phase sensitive, lock-in detection technique. With careful control of the beam walk, the resolution of $\Delta T/T$ is about 10^{-6} for the single modulation and 10^{-7} for the double modulation technique. The maximum time delay between the pump and probe pulses was 2 ns with a resolution of 100 fs. In order to avoid excessive photooxidation, all measurements at room temperature were done in either a dynamic vacuum or N₂ flow. We also performed measurements at lower temperatures using a liquid nitrogen cryostat. With the polarization of the probe and pump beams 45° to each other, ΔT_{\parallel} and ΔT_{\perp} were measured when the analyzer was set to be parallel or perpendicular to the polarization of the pump beam, respectively. The polarization memory P as defined in the following relation:

$$P = \frac{\Delta T_{\parallel} - \Delta T_{\perp}}{\Delta T_{\parallel} + \Delta T_{\perp}} \quad (1)$$

was calculated up to 2ns and thus its decay was also studied.

Our measurements were done on thin polymer films of thickness 1 μm or less. We dissolved 6 mg Si-PT powder into 2 ml xylenes (C₆H₄(CH₃)₂) and then evaporated the solution on transparent quartz substrates. To get a Si-PT film, this procedure was repeated several times till the required thickness was obtained. The same preparation method was also applied to s-CH)_x.

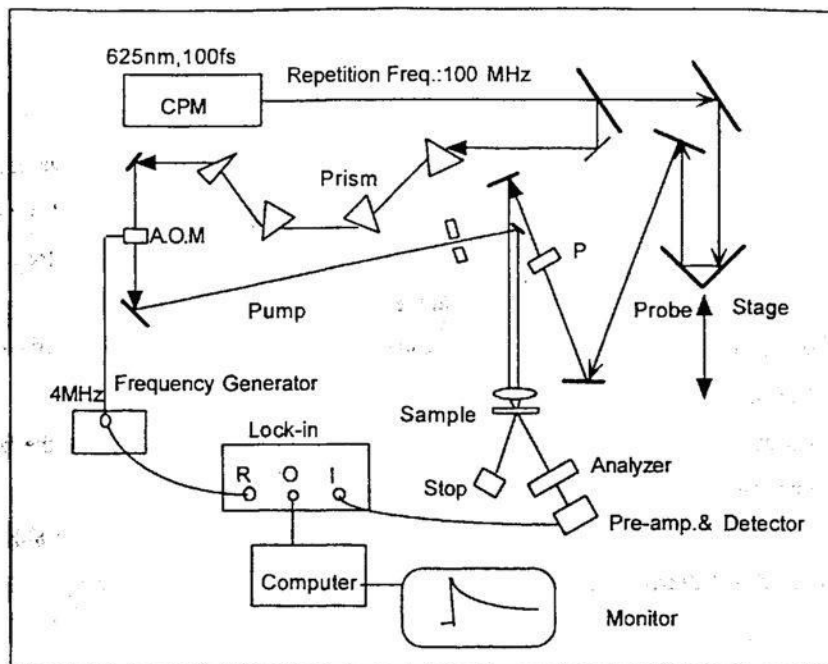


Fig.1. (a) Single modulation configuration
A.M.O.-Acousto-Optic Modulator

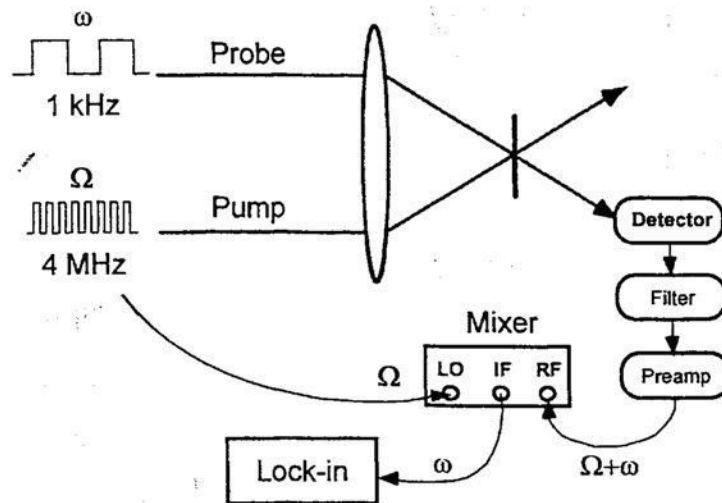


Fig.1 (b) Double Modulation Configuration

3. EXPERIMENTAL RESULTS:

I: Si-PT.

Fig.2 shows typical absorption and PL spectrum of a Si-PT film, from which we estimate that the optical gap, E_g , is about 1.8 eV. Correspondingly, the PL band spans from 1.3 eV to 1.8 eV. The polymer repeat unit is also shown in the inset. We note that the absorption peak is conveniently located at 2.1 eV, so that the CPM laser excitation at 2.0 eV is almost at the absorption maximum (Fig. 2).

Fig.3 shows the decay dynamics of $(\Delta T/T_{\parallel})$ and $(\Delta T/T_{\perp})$ as well as $P(t)$ in a Si-PT film at different time scales measured at 300K. The P decay characterizes the transport properties of the observed photoexcitations assuming that the decay of P can occur only through the drift of the photoexcitations along the polymer chains (sometimes enhanced by inter-chain hopping). Fig. 4 summarizes $\Delta T/T$ decay at different time scales on a logarithm scale. We also measured $\Delta T/T$ in Si-PT films at 80K and 140K and observed similar $\Delta T/T$ decays to those at room temperature.

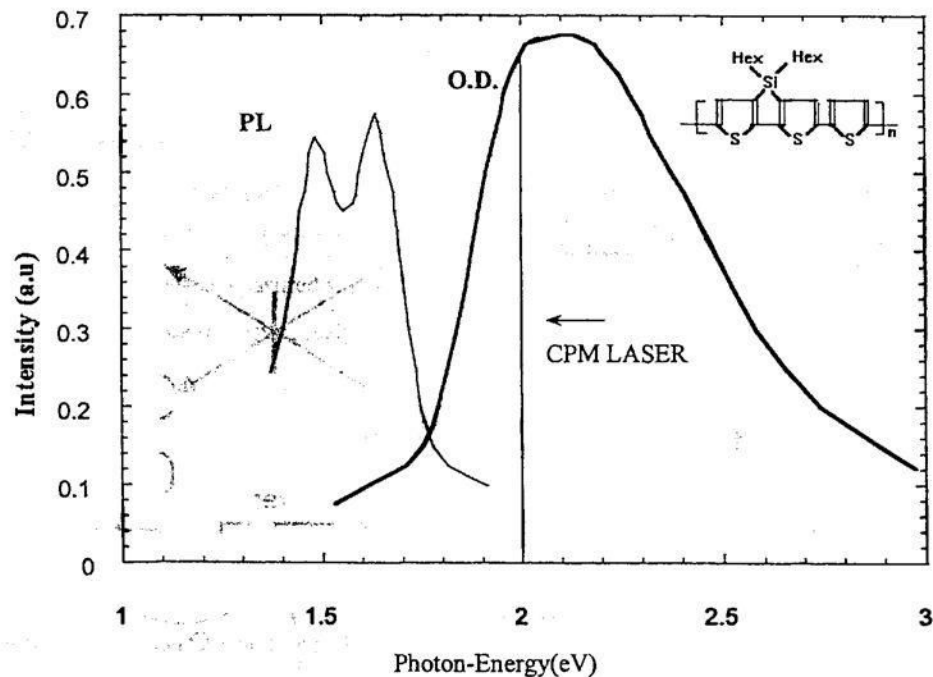


Fig.2. Optical Absorption and Photoluminescence Spectrum of Si-PT

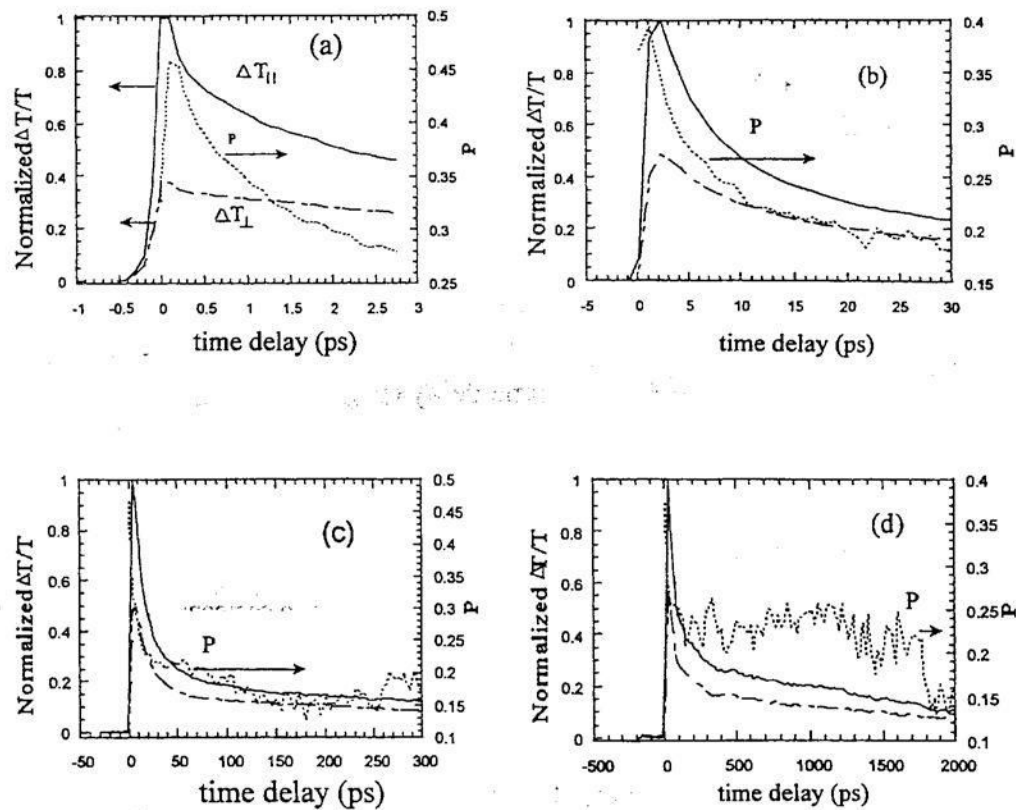


Fig.3. ($\Delta T/T_{||}$) (full lines), ($\Delta T/T_{\perp}$) (long dash lines) and Polarization memory (dotted lines) decays in Si-PT at 300K, on different time scales ranging from 3ps to 2000ps.

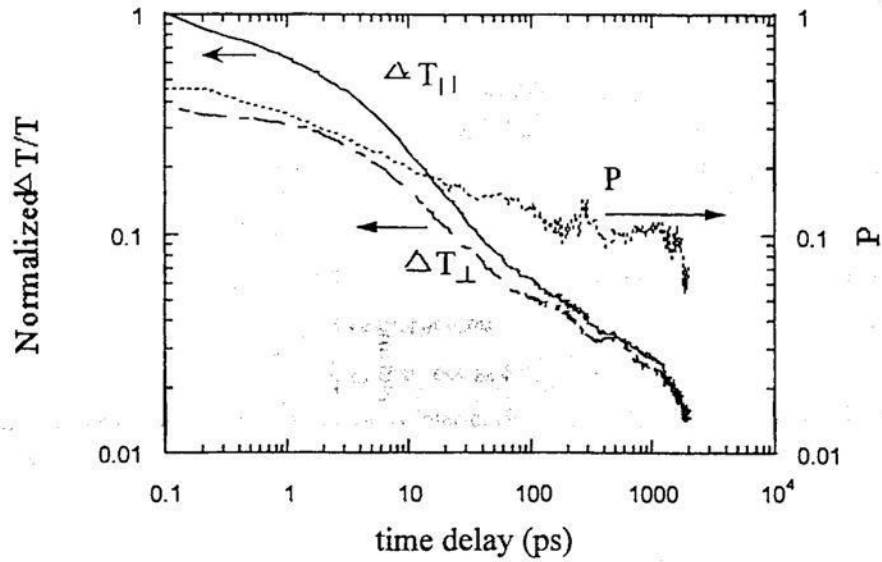


Fig.4. Ps photoresponse dynamics in Si-PT at 300K.

It is quite apparent in Fig.4 that each response decay has at least two components with different time constants. We therefore tentatively attribute $\Delta T/T$ decay to two successive photoexcitation relaxation processes and fit the data with a biexponential function as follows

$$\Delta T / T = a \cdot \exp(-t / T_1) + b \cdot \exp(-t / T_2) + c \quad (2)$$

where a , b , c are three free fitting parameters, and T_1 and T_2 are two characteristic time constants.

Fig. 5 (a) and (b) show $\Delta T_{||}/T$ decays and their fits at 300K and 80K, respectively. It is apparent that the decay dynamics is temperature independent. Fig. 5 (c) shows $P(t)$ at these two temperatures. We conclude from $P(t)$ decay temp. dependence show that the excitons in Si-PT have temperature dependent transport properties : since at 300K, polarization memory decays much faster than at 80K. Table 1 lists the various decay time constants of Si-PT films at different temperatures; it can be seen that $T_1 \sim 5$ ps and $T_2 \sim 50$ ps.

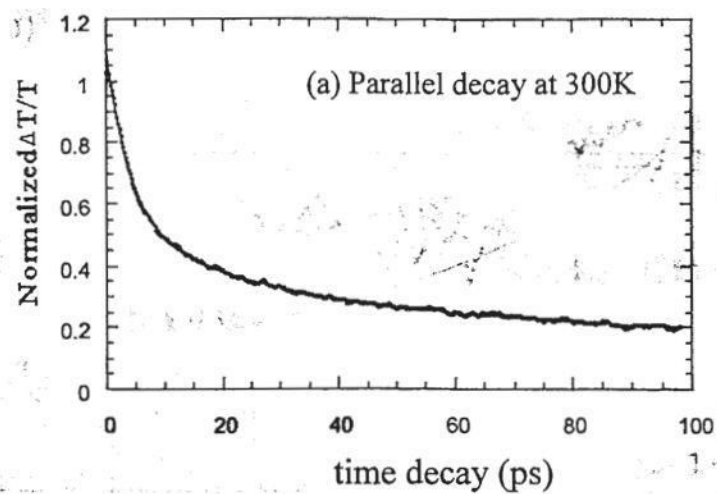


Fig.5. (a) ΔT_{\parallel} decay at 300K (dotted line) and its fit (full line).

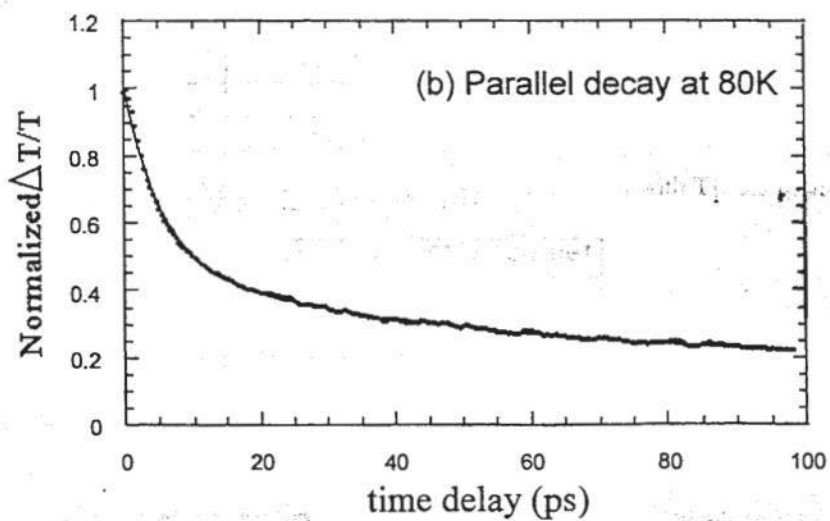


Fig.5. (b) ΔT_{\parallel} decay at 80K (dotted line) and its fit (full line).

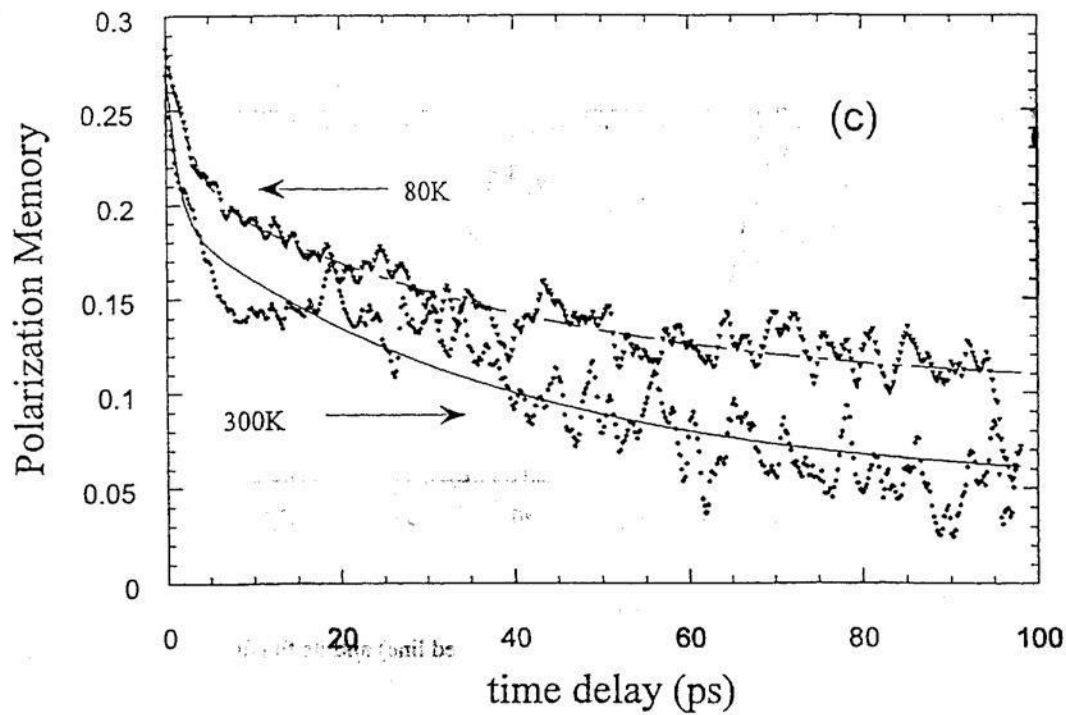


Fig.5. (c) Polarization memory decay at 80K and 300K (dotted lines) and their fits with Eq.(2).

(a) parallel component

temperature(K)	T1 (ps)	T2 (ps)
80	5.2	52
140	5.1	39
300	5.7	49

(b) perpendicular component.

temperature(K)	T1 (ps)	T2 (ps)
80	5.4	55
140	5.6	49
300	6.2	55

(c) Polarization memory

temperature(K)	T1(ps)	T2(ps)
80	2.7	41
140	1.4	36
300	1.3	39

Table 1 Decay time constants of Si-PT at different temperatures.

Fig. 6 shows the intensity dependence of the PM decay. In the experiments, we reduced the pump beam intensity while keeping the probe beam intensity unchanged. We can see that the PM decay is intensity independence. We therefore conclude that the recombination dynamics (T_2) is linear, whereas the ultrafast decay (T_1) is intrinsic to polymers.

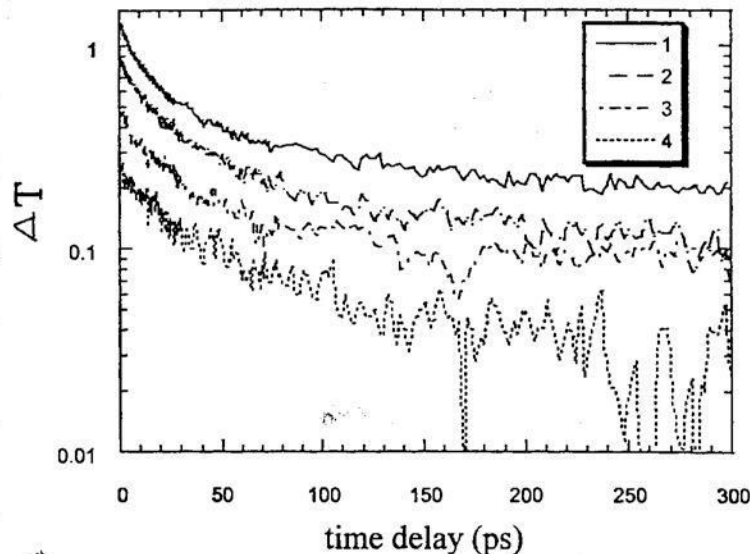


Fig. 6. Intensity dependence of ΔT_{\perp} .
The initial photoexcitation density given in units of $10^{17}/\text{cm}^3$ are: (1)-4; (2)-3; (3)-2; (4)-1.

$\Pi : s-(\text{CH})_X$

Fig. 7. (a) shows a typical optical absorption spectrum of the nonluminescent $s-(\text{CH})_X$, whereas Fig. 7.(b) shows $\Delta T/T$ decay up to 8 ps. We also fit ΔT decay using Eq.(2) with $T_1 \sim 0.5$ ps and $T_2 \sim 5$ ps as shown in Fig. 7. (b))(6).

4. DISCUSSION

We note that at 2.0 eV $s-(\text{CH})_X$ exhibits photo induced absorption (PA), i.e. $\Delta T/T < 0$, whereas Si-PT shows photo-bleaching (PB), i.e. $\Delta T/T > 0$. This can be understood when looking at their different optical absorption spectra given in Fig. 2 and 7 (a), respectively. It is generally accepted that fs laser excitation results in two major optical effects at $\hbar\omega$ close to the optical gap: (i) photo bleaching of the ground state absorption and (ii) red shift of the optical absorption spectrum due to phonon emission, which results in excess population of the ground state high vibronic levels.

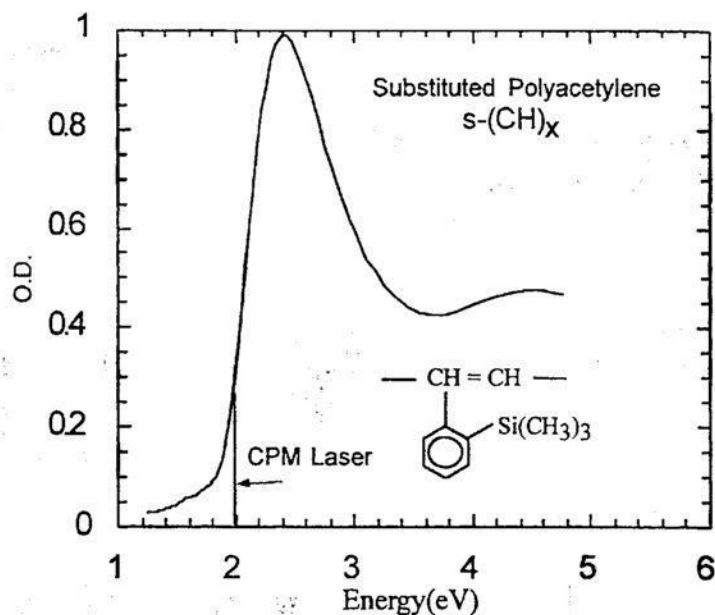


Fig.7 (a) Optical absorption spectrum of $s\text{-(CH)}_x$ and its backbone.

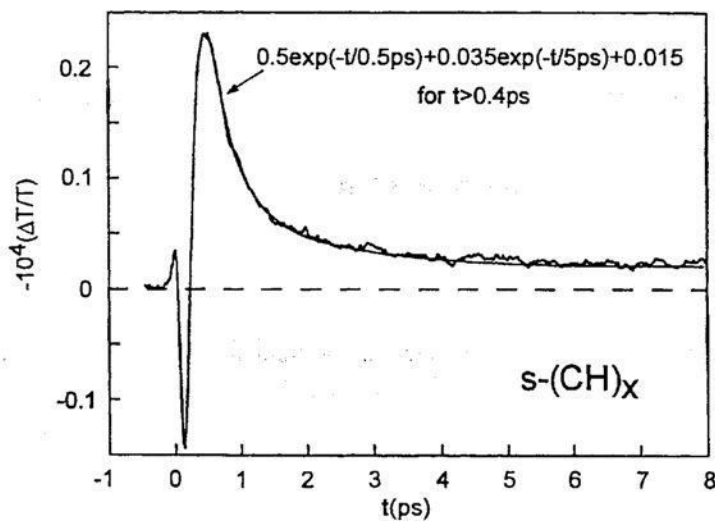


Fig.7 (b) Ultrafast ΔT decay in $s\text{-(CH)}_x$ at 300K.

As shown in Fig.8 (a) for $s\text{-(CH)}_x$, the spectral red shift causes the increase of the absorption coefficient at 2.0 eV, which overcomes the effect of the photo bleaching. However, in Si-PT, since the probe energy is very close to the absorption maximum, the bleaching effects prevails. This may explain the different signs of ΔT at 2.0 eV observed in these two films.

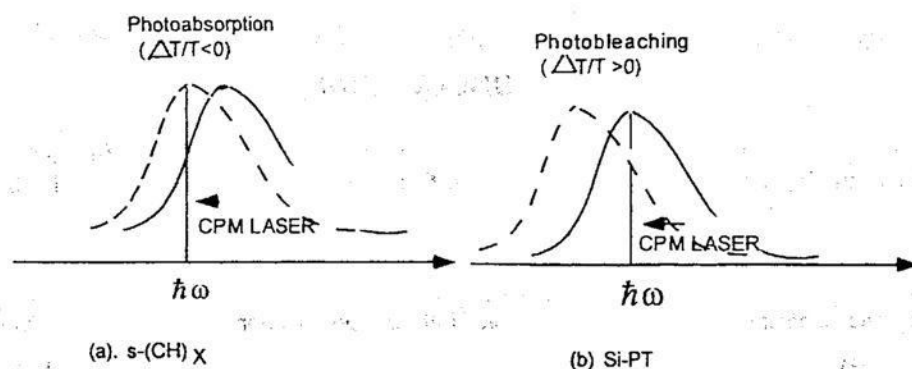


Fig. 8. Red-shift of absorption spectra of conducting polymers.

We can also see that ΔT decays in $s\text{-(CH)}_X$ are much shorter than those in Si-PT. If we relate T_1 to the thermalization and internal conversion processes, and T_2 to recombination, then the possible key to understanding this difference in dynamics is the parity of the lowest excited states. As shown in Fig.9, the ground state, $1A_g$ has an even parity and the excited states may have even or odd parities ($2A_g$ or $1B_u$) respectively depending on whether the polymer is nonluminescent or luminescent. Since the optical transitions are allowed only between states of opposite parity, such optical transitions can occur only between A_g and B_u states. In Si-PT, the $1B_u$ exciton is below $2A_g$, and the dynamics in these samples is dominated by the radiative recombination channel. On the contrary, in $s\text{-(CH)}_X$, the lowest excited state is expected to be $2A_g$, which has the same parity as the ground state and, therefore, the optical transition between these two states is dipole forbidden. It requires a new relaxation channel, i.e. phonons emission, to release the excess energy received by the exciton system from the pump pulse. In this case, the non-radiative emission of the strongly coupled A_g Raman active modes may then explain the ultrafast T_2 relaxation dynamics of this sample.

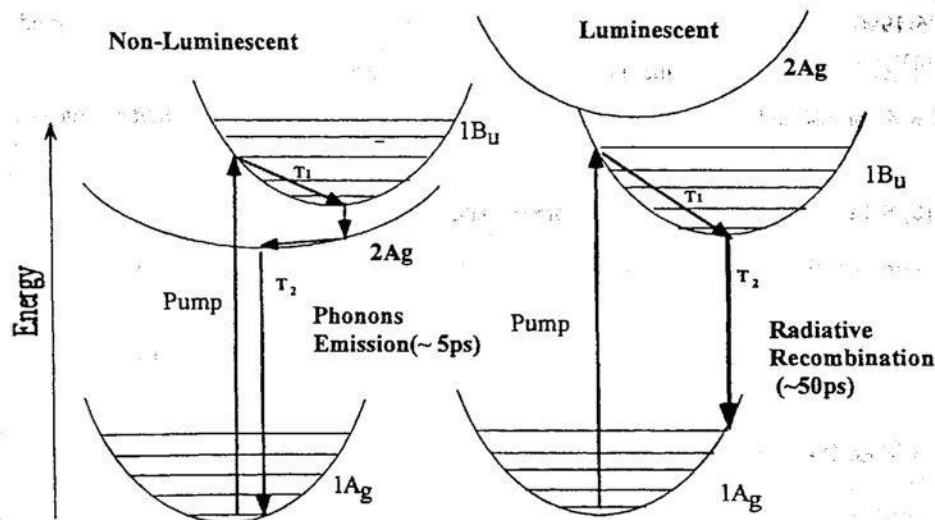


Fig. 9. The schematic energy states and optical transitions of nonluminescent and luminescent conducting polymers

5. CONCLUSIONS

We have studied the fs to ns photorelaxation dynamics in a luminescent sample, Si-PT, and nonluminescent sample, s-(CH)_x in the low signal limit. In Si-PT, we identify two decay processes with time constants $T_1 \sim 5$ ps and $T_2 \sim 50$ ps, respectively. We also see that ΔT decay has no obvious temperature and intensity dependences and that at 300K the polarization memory decays faster than at 80K. In s-(CH)_x, we also identify two decay processes, with $T_1 \sim 0.5$ ps and $T_2 \sim 5$ ps, which are much shorter than in Si-PT.

We tentatively relate T_1 to the thermalization and internal conversion processes and T_2 to recombination and, therefore, attribute the difference in T_2 between Si-PT and s-(CH)_x to radiative versus non-radiative recombination dynamics in these two polymers.

6. ACKNOWLEDGMENTS:

This work was supported in part by the DOE grant # : FG-03-96-ER 45490.

7. REFERENCES:

- [1] Z.G.Soos, S.Ramasesha, and D.S.Galvao, Phys. Rev. Lett. 71, 1609, (1993).
- [2] W.Chen, Ph.D. thesis, 8/97, Ames Laboratory, Iowa (Unpublished).
- [3] A.F.Brassett, N.F.Colaneri, D.D.C.Bradley, R.A.Lawmnce, R.H.Friend, H.Murata, Phys.Rev.B41, 10586(1990)
- [4] Z.V.Vardeny and J.Tauc, in Semiconductors Probe by Ultrafast Laser Spectroscopy, V.2, edited by R.R.Alfano (Academic Press, 1984).
- [5] S.V.Frolov, Ph.D. thesis, 1996, University of Utah (unpublished) .
- [6] S.Takeuchi, T.Masuda, T.Higashimura, and T.Kobayashi, Solid State Comm. 87, 655(1993).